AAS 22-692

TIME-VARYING PERTURBATION MODEL IDENTIFICATION IN THE NEIGHBORHOOD OF CR3BP PERIODIC ORBITS

Matthew Brownell[*], Damien Guého [†], Roshan Eapen[‡], Puneet Singla[§]

The main focus of this work is to find a linear, time-varying model to capture the dynamics of periodic solutions in the vicinity of Lagrange points in the Earth-Moon system via position and velocity measurements. This is motivated by a need for station keeping in said orbits. Rather than finding a global model between input and output space, subspace methods for linear system identification will be utilized to find a subspace over which the unknown dynamics evolve. This identification method allows one to obtain a simplified linear model that deals with dominant dynamics of the system, and subsequently apply known control theory for station keeping.

INTRODUCTION

The Global Exploration Roadmap[1,10,14,27] has garnered a renewed interest in the exploration of the solar system. Among several different efforts, NASA is currently focused on positioning and maintaining an inhabited facility in a long-term and relatively stable orbit in the lunar vicinity. The Earth-Moon libration points offer many options for both the storage of propellant and supplies for lunar missions, as well as potential locations for a space-based facility to support future crewed and robotic translunar missions.[10,27] Envisioning a larger traffic of space missions fueled by Artemis' plan of expanding the nation's geo-strategic and economic sphere to encompass the Moon with international partners and private industry, applied research into autonomous guidance, navigation, and control, autonomous re-planning, and expanding the knowledge base of possible transport opportunities within the expanded Earth neighborhood is warranted.

The pioneering work by Conley[2] on the existence of transit trajectories in the Planar Circular Restricted Three Body Problem (PCR3BP) led to much attention being devoted to leveraging the collinear points for space missions.[3,4,11,16,17,26] The collinear equilibrium points host a variety of different families of periodic solutions in its vicinity. The family of periodic orbits in the vicinity of the L_1 and L_2 points exhibit both stable and unstable behavior. A particular class of three-dimensional periodic orbits, called the Near Rectilinear Halo Orbits (NRHO) are shown to be stable periodic orbits under the framework

[*]Graduate Student, Department of Aerospace Engineering, The Pennsylvania State University, University Park, PA, 16802

[†]Graduate Student, Department of Aerospace Engineering, The Pennsylvania State University, University Park, PA, 16802

[‡]Assistant Professor, Department of Aerospace Engineering, The Pennsylvania State University, University Park, PA, 16802

[§]Professor, AIAA Associate Fellow, AAS Fellow, Department of Aerospace Engineering, The Pennsylvania State University, University Park, PA, 16802

of the CR3BP. Therefore, one can reasonably assume that in a higher fidelity dynamical framework, the external perturbations will will not result in a significantly large deviation from the nominal halo orbit. Over an extended period of time, the perturbed motion may remain arbitrarily close to the nominal solution due to the inherent stability of the periodic solution.

Assuming inertial measurements are available for a spacecraft located in an NRHO, and treating them as the output of a dynamical system, this work proposes to utilize the system identification tool the Eigensystem Realization Algorithm (ERA) to find the subspace over which the dynamics can be explained while approximating the input-output data with a linear, time-varying system. Using the data-approximated state transition matrix, a station-keeping strategy is developed that uses active control to bring the spacecraft back to the nominal trajectory. This subspace will be in the form of a linear, time-varying system that is least square based and is valid in a larger domain than the conventional Taylor series based linearization.

Previous work with Koopman Operators approximates the dynamics near Lagrange points instead as a linear, time-invariant system in a very high dimensional space.[22] In general, one wishes to have the approximated system be low dimensional for performance reasons. High dimensionality generally means the model is not be amenable to analysis and control. In addition, the relationship between eigenvalues of the Koopman operator and the true dynamical characteristics are often difficult to understand. When utilizing the identified system found via ERA, the dimension is low and the eigenvalues are easier to understand.

In this paper, the dynamics of the CR3BP will be briefly discussed, the station-keeping method will be outlined, and the corresponding data-driven modeling algorithm (ERA) will be discussed. Lastly, the validity of the data-driven model in the context of the CR3BP will be tested.

PROBLEM STATEMENT

The motion of a particle subjected to the gravitational attraction of two bodies (i.e., primaries) is studied in this work.[8,19,24] The underlying assumption that the mass of the particle is negligible compared to the primary masses allows treatment of the three-body problem as restricted in the sense that the primaries are assumed to move on Keplerian orbits around their common barycenter. In this work, a special case of the restricted three-body problem is considered wherein the primaries move in circular orbits. This dynamical model is known as the Circular Restricted Three-Body Problem (CR3BP). It is described using the vector differential equation below.

$$\ddot{\mathbf{q}} + 2\omega \times \dot{\mathbf{q}} = \frac{\partial \Omega}{\partial \mathbf{q}} \tag{1}$$

where, $\omega = [0, 0, n]^T$ and $\mathbf{q} = [x, y, z]^T$. $\Omega = \frac{1}{2}(x^2 + y^2) + \frac{1-\mu}{r_1} + \frac{\mu}{r_2}$ is the CR3BP pseudo-potential obtained by augmenting the inertial potential with the potential of the rotating frame. Then, $r_1 = ((x + \mu)^2 + y^2 + z^2)^{1/2}$ and $r_2 = ((x - 1 + \mu)^2 + y^2 +$

$z^2)^{1/2}$ locate the third body with respect to the first and second primary, respectively. It is conventional to nondimensionalize the quantities in the CR3BP by selecting characteristic quantities: the distance between the two primaries, and the sum of their masses are chosen as units of length and mass.[18,24] The characteristic time is determined by normalizing the mean motion, n, which gives the value of the gravitational constant as unity. Therefore, the primaries complete one revolution about their barycenter in time $t = 2\pi$. The mass parameter is defined as $\mu = \frac{m_2}{m_1+m_2}$. Note that $\mathbf{q}$ is described in a rotating frame. The transformations to the inertial frame coordinates ($\mathbf{Q} = [X, Y]$) are obtained through a simple rotation about ω by an angle θ such that $\dot{\theta} = 1$.[24] This geometrical formulation is illustrated in Figure 1.

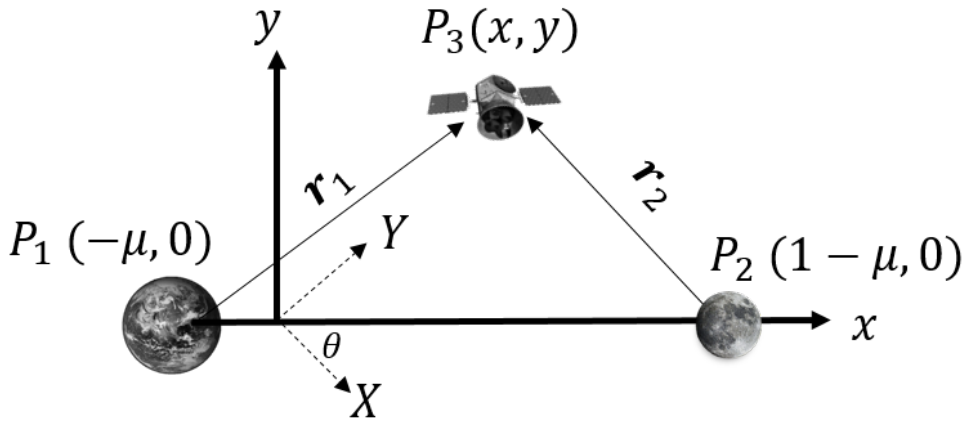

Figure 1: Geometrical formulation for the PCR3BP. P_1 and P_2 are the two primaries with masses, m_1 and m_2, respectively. P_3 is the third body, located at (x, y) in the rotating frame.

The equations of motion for the CR3BP are written more generally as,

$$\dot{\boldsymbol{x}} = \boldsymbol{f}(\boldsymbol{x}) \tag{2}$$

where $\boldsymbol{x} = [x, y, z, \dot{x}, \dot{y}, \dot{z}]^T$. Consider any nominal trajectory that one wishes to station keep around, denoted as $x_{Nom}(t)$. If the true motion of the spacecraft is given by $x(t)$, then the true perturbation from the nominal is

$$\delta\boldsymbol{x}(t) = \boldsymbol{x}(t) - \boldsymbol{x}_{Nom}(t) \tag{3}$$

If we instead preform a Taylor series expansion about the nominal trajectory and neglect higher-order terms, the following approximation of the perturbation dynamics is obtained:

$$\dot{\delta\tilde{\boldsymbol{x}}} = A(\boldsymbol{x})\delta\tilde{\boldsymbol{x}} \tag{4}$$

$$A(\boldsymbol{x}) = \left.\frac{\partial \boldsymbol{f}}{\partial \boldsymbol{x}}\right|_{Nom} \tag{5}$$

where $\delta\tilde{\boldsymbol{x}}$ is the perturbation from the nominal orbit obtained via the linearization and $A(\boldsymbol{x})$ is the Jacobian of the nonlinear system. This linearized equation can then be discretized as,

$$\begin{aligned} 692\delta\tilde{\boldsymbol{x}}_{k+1} &= \Phi(k+1,k)\delta\tilde{\boldsymbol{x}}_k \\ &:= A_k\delta\tilde{\boldsymbol{x}}_k \end{aligned} \tag{6}$$

This linearization provides a good approximation around the neighborhood of the nominal orbit, but will degrade once the state is sufficiently far from the nominal. To obtain $\Phi(k+1,k)$, one must integrate the following differential equation between time steps (k to $k+1$):

$$\dot{\Phi} = A(\boldsymbol{x})\Phi \tag{7}$$

In the case of the nominal being a point instead of a trajectory, $A(\boldsymbol{x})$ is constant and $\Phi = exp(A(\boldsymbol{x})\Delta t)$.

Description of Dynamics

The goal of this paper is to utilize time-varying ERA (TVERA) to identify the A_k matrix using inertial position and velocity measurements over some time period. The reference value of A_k can be computed using the true dynamics of equation (7). In general, these measurements can be obtained from inertial measurement units (IMUs) onboard or high fidelity ephemeris models offline. For simplicity, the measurements used in this paper will be obtained by propagating initial conditions found by perturbing the nominal orbit's initial condition.

In this paper, we will consider station keeping around a nominal NRHO. First, the nominal initial condition, $\boldsymbol{x}_{Nom}(0)$, is perturbed to obtain N perturbed initial conditions denoted as $\boldsymbol{x}^i(0)$. These new initial conditions are then propagated for one nominal orbital period to obtain N perturbed orbits. Based off equation (3), the perturbation from the nominal is then,

$$\delta\boldsymbol{x}^i(t) = \boldsymbol{x}^i(t) - \boldsymbol{x}_{Nom}(t) \tag{8}$$

where $i = 1, 2, ...N$.

This results in the true perturbation motion that will be used for the system identification process. The linearized equation (6) provides the reference for the linear perturbation dynamics of the nominal orbit. This reference will then be compared to the identified linear model obtained via TVERA, denoted as $\delta\hat{\boldsymbol{x}}$.

There are now three different perturbation models: perturbations found via the true nonlinear dynamics, $\delta\boldsymbol{x}$, true linearized dynamics, $\delta\tilde{\boldsymbol{x}}$, and identified linear dynamics, $\delta\hat{\boldsymbol{x}}$. This paper studies two aspects of station-keeping with system identification: (1) Compare the identified linear dynamics with the true linearized dynamics in the reproduction of the CR3BP nonlinear dynamics in the perturbation region of the NRHO, and (2) test if the identified system can be utilized for station keeping about the nominal NRHO.

Fixed-Time Targeting Problem

In order to test the applicability of the identified system for station keeping, we consider a standard impulsive velocity maneuver that is found using differential corrections. In general, in a fixed-time targeting problem one is given an initial state, a desired state on the orbit, and a fixed time-of-flight. The goal is to calculate the required impulsive change in initial velocity, ΔV, so that the desired state is reached in the fixed time-of-flight.

In order to solve for this ΔV, an iterative process is performed. This process is outlined below:

1. Propagate the initial perturbed state for the given time-of-flight with an initial guess for ΔV
2. Calculate the error between the final state and desired state
3. Utilize the state-transition matrix $\Phi(t_{final}, t_{initial})$ to calculate an updated ΔV
4. Adjust the initial state of the current iteration with updated ΔV
5. Repeat until a user-defined tolerance is met

One can calculate ΔV using the following least squares solution,

$$\Delta V = P^{\dagger}(X_{final} - X_{Desired}) \tag{9}$$

$$P = \begin{bmatrix} \Phi_{rv} \\ \Phi_{vv} \end{bmatrix} \tag{10}$$

$$\Phi(t_{final}, t_{initial}) = \begin{bmatrix} \Phi_{rr} & \Phi_{rv} \\ \Phi_{vr} & \Phi_{vv} \end{bmatrix} \tag{11}$$

where $(.)^{\dagger}$ denotes a pseudo inverse. The state-transition matrix Φ (arguments dropped for simplicity) can be found at any time by integrating equation (7) alongside the nonlinear dynamics given by equation (2), where the initial condition of Φ is the identity matrix. Note that $A(\boldsymbol{x})$ is the Jacobian of the nonlinear system and is linearized about the perturbed trajectories found during each iteration of the differential corrections process enumerated above. This differential equation for Φ will be taken as the ground-truth for the differential corrections process in this paper. The methodology of differential corrections for the identified system found via TVERA is explained in the next two sections.

METHODOLOGY

In this section the mathematical framework for ERA is developed. Making use of input/output data, a Singular-Value Decomposition provides a low-fidelity model for a dynamical system. Additionally, the comparison of eigenvalues and transformation of coordinate frames is also discussed.

The Eigensystem Realization Algorithm (ERA)

This paper utilizes the linear system identification tool, the Eigensystem Realization Algorithm (ERA),[12,13] to find the subspace over which the dynamics can be explained while approximating the input-output data collected from position and velocity sensors. In essence, this paper aims to identify a linear model that captures the dominate modes of system when perturbed from a nominal orbit. In general, the output of a system at any given time is considered a function of the input signal, and the input signal is a function of time. Implicitly, one hopes the input-output data approximated is sufficiently rich that the model will be accurate over a wide class of inputs, and is useful for other purposes such as station-keeping. ERA provides a minimal-realization of the system based solely off input/output data and allows for further system analysis and control. The specific problem of orbit control blends concepts from engineering mechanics, control theory, and computational science in order to keep the spacecraft in a desired orbit. Working at the confluence of these different disciplines, the engineers of this era contributed to many advancements in linear system theory. As a result, the proceeding decades led to many works in the time-domain identification of linear systems.[9,20,21,23,25] Soon after, Ho and Kalman[9] paved the way for minimum realization theory by showing that a minimum dimension state space model can be achieved by analyzing a sequence of pulse response functions known as Markov parameters. Since then, an extension of the Ho-Kalman algorithm, known as the Eigensystem Realization Algorithm (ERA),[12,13] has been at the forefront of system identification due to its efficiency and ease of use. In short, ERA constructs a Hankel matrix from the pulse response functions and utilizes the Singular-Value Decomposition to realize the minimum order of the system. The low dimensionality of the dynamic map identified through ERA is of interest given the corresponding low computational complexity.

Time-Varying ERA from Initial Condition Response

Given that the true linear perturbation dynamics, given by equation (4), have a time-varying system matrix, it is reasonable to assume the identified system should be time varying as well. TVERA is an algorithm that requires either data from zero initial condition with impulse input or nonzero initial condition with zero input.[5–7,15] In this paper, we will preform the initial-condition response (referred to as TVERA/IC) on the orbital data obtained from position and velocity sensors. System matrix $\hat{A}_k$, output matrix $\hat{C}_k$, and initial condition vector $\hat{X}_0$ will be the output of TVERA/IC. The $\hat{X}_0$ vector is a vector of our initial conditions in the minimal-realization coordinate system (also referred to as the identified system). This minimal coordinate system has no physical meaning. The response of a generic discrete system with no input and an arbitrary initial condition (may be nonzero) is

$$\boldsymbol{x}_{k+1} = A_k \boldsymbol{x}_k \tag{12}$$

$$\boldsymbol{y}_k = C_k \boldsymbol{x}_k \tag{13}$$

The general solution of equations (12) and (13) can be written in terms of the state-

transition matrix, Φ_k, as,

$$\boldsymbol{x}_k = \Phi(k, k_o)\boldsymbol{x}_0 \tag{14}$$

$$\boldsymbol{y}_k = C_k\Phi(k, k_o)\boldsymbol{x}_0 \tag{15}$$

where $\Phi(k, k_o)$ is defined as,

$$\Phi(k, k_o) = \begin{cases} A_{k-1}A_{k-2}...A_{k_0}, & \forall k > k_0 \\ I & k = k_0 \\ undefined, & \forall k < k_0 \end{cases} \tag{16}$$

We are interested in gathering information about the system from the initial condition response data. The concept of observability is still valid, with the observability matrix defined as

$$O_k^{(p)} = \begin{bmatrix} C_k \\ C_{k+1}A_k \\ C_{k+2}A_{k+1}A_k \\ \cdots \\ C_{k+p-1}A_{k+p-2}...A_0 \end{bmatrix}. \tag{17}$$

We now define a Hankel-like matrix, $\tilde{H}_k$, whose columns consist of N experimental data vectors. These N columns of output data are concatenated up to the $(k+p-1)^{th}$ time step, where p and N are chosen by the user to capture the order, n, of the system.

$$\tilde{H}_k^{(p,N)} = \begin{bmatrix} y_k^{\#1} & y_k^{\#2} & \cdots & y_k^{\#N} \\ y_{k+1}^{\#1} & y_{k+1}^{\#2} & \cdots & y_{k+1}^{\#N} \\ \vdots & \vdots & \ddots & \vdots \\ y_{k+p-1}^{\#1} & y_{k+p-1}^{\#2} & \cdots & y_{k+p-1}^{\#N} \end{bmatrix} \tag{18}$$

To obtain a minimum realization of the discrete system, we perform a singular value decomposition of the $\tilde{H}_k$ matrix. The minimal coordinate system mentioned before is a result of this decomposition.

$$\tilde{H}_k = O_k^{(P)}X_k^{(N)} = U_k\Sigma_k^{\frac{1}{2}}\Sigma_k^{\frac{1}{2}}V_k^T \tag{19}$$

$$= \begin{bmatrix} U_k^{(n)} & U_k^{(0)} \end{bmatrix} \begin{bmatrix} \Sigma_k^{(n)} & 0 \\ 0 & \Sigma_k^{(0)} \end{bmatrix} \begin{bmatrix} V_k^{(n)^T} \\ V_k^{(0)^T} \end{bmatrix} \tag{20}$$

$$\simeq U_k^{(n)}\Sigma_k^{n^{\frac{1}{2}}}\Sigma_k^{n^{\frac{1}{2}}}V_k^{(n)^T} \tag{21}$$

Then, it can be shown that a minimum realization of the discrete system is given by

$$\hat{A}_k = \Sigma_{k+1}^{n^{\frac{1}{2}}}V_{k+1}^{(n)^T}V_k^{(n)}\Sigma_k^{n^{-\frac{1}{2}}} \tag{22}$$

$$\hat{C}_k = E^{(m)^\top}U_k^{(n)}\Sigma_{k+1}^{n^{\frac{1}{2}}} \tag{23}$$

$$\hat{X}_0 = \Sigma_0^{n^{-\frac{1}{2}}}U_0^{(n)^T}\tilde{H}_0 \tag{24}$$

where $E^{(m)^T} = \begin{bmatrix} I_m & O_m & \dots & O_m \end{bmatrix}$ and m is the number of outputs for each experiment. We can now utilize equations (22)-(24) within equations (12) and (13) to iterate over time and reproduce the given output data. It is important to emphasize that the corresponding state obtained via the singular value decomposition is not generally the same as the true state. In this paper, the identified system's state is denoted as $\boldsymbol{z}$ and the position/velocity state is denoted as $\boldsymbol{x}$. Note that one can only identify the model until the time step $t_f - p$. Any time after $t_f - p$, the $\tilde{H}_k$ matrix cannot be filled out and thus a state-space realization cannot be obtained. This meaning, the larger the value of p, the less time the identified model is valid for.

Comparing Identified and Reference Eigenvalues

One can write a transformation from the traditional position/velocity state vector $\boldsymbol{x}$ to a new state vector, $\boldsymbol{z}$, as,

$$\boldsymbol{z}_k = T_k \boldsymbol{x}_k \tag{25}$$

where $\boldsymbol{z}$ is the minimal realization coordinate system state vector obtained via TVERA (also referred to in this paper as the 'identified' or 'minimal' state). Rewriting equation (12) in terms of $\boldsymbol{z}$,

$$\begin{aligned} \boldsymbol{z}_{k+1} &= T_{k+1}^{-1} A_k T_k \boldsymbol{z}_k & (26) \\ &:= \hat{A}_k \boldsymbol{z}_k & (27) \end{aligned}$$

Note here that, unlike in time-invariant systems, $\hat{A}_k$ is not a similarity transformation of A_k; it is a more generic, topological transformation of A_k. This implies that the system matrices $\hat{A}_k$ and A_k do not have the same eigenvalues at any arbitrary values of k. Because the system evolution takes place in two different coordinate systems, T_{k+1}, T_k, this leads the basis vectors for the initial time step and the final time step to be different. We wish to compare the eigenvalues of the true and identified system matrices for analysis purposes. This discrepancy can be corrected by applying the following correction to the system matrix,

$$\tilde{\hat{A}}_k = O_k^{\dagger} O_{k+1} \hat{A}_k \tag{28}$$

where $(.)^{\dagger}$ denotes a pseudo inverse. Equation (28) shows the transformation for the identified system matrix, $\hat{A}_k$, but this transformation must be applied to the true system matrix, A_k, as well. After the above transformation is applied, the following occurs:

$$\begin{aligned} \tilde{\hat{A}}_k &= O_k^{\dagger} O_{k+1} \hat{A}_k \\ &= T_k^{-1} O_k^{\dagger} O_{k+1} T_{k+1} T_{k+1}^{-1} A_k T_k \\ &= T_k^{-1} \underbrace{O_k^{\dagger} O_{k+1} A_k}_{\tilde{A}_k} T_k \\ &= T_k^{-1} \tilde{A}_k T_k \end{aligned}$$

After the transformation, the system matrices are similarity transformations of each other and their eigenvalues can be compared at each time step. If the true system is a time-varying, linear system, then the true and identified eigenvalues should match post transformation. If the true system is nonlinear, then the eigenvalues do not necessarily match. In this paper, we are dealing with a nonlinear system but still wish to see how the eigenvalues compare post transformation.

Converting from Identified to True Coordinate System

In general, there is no guarantee that one will be able to convert the identified system matrix, $\hat{A}_k$, to the true system matrix, A_k. It heavily depends on how well conditioned your identified output matrix, $\hat{C}_k$, is. In general, the identified system is written as,

$$\begin{aligned} \boldsymbol{z}_{k+1} &= \hat{A}_k \boldsymbol{z}_k \\ \boldsymbol{x}_k &= \hat{C}_k \boldsymbol{z}_k \end{aligned}$$

By modifying indices and doing some algebraic manipulation, one can write the following formulation,

$$\begin{aligned} \boldsymbol{x}_{k+1} &= \hat{C}_{k+1} \hat{A}_k \hat{C}_k^{-1} \boldsymbol{x}_k \\ &= A_k \boldsymbol{x}_k \end{aligned}$$

Therefore,

$$A_{k,est} = \hat{C}_{k+1} \hat{A}_k \hat{C}_k^{-1} \tag{29}$$

We now have a direct way to calculate our estimation of the true system matrix, A_k, from our identified system and output matrices. Due to the inversion of $\hat{C}_k$, the conversion is dependent upon the identified system output matrix being nonsingular (can do least squares or minimum norm solution if nonsquare).

SOLUTION APPROACH

After preforming TVERA/IC the following system will be identified,

$$\delta \boldsymbol{z}_{k+1} = \hat{A}_k \delta \boldsymbol{z}_k \tag{30}$$

$$\delta \hat{\boldsymbol{x}}_k = \hat{C}_k \delta \boldsymbol{z}_k \tag{31}$$

where $\hat{A}_k$ is the identified system matrix, $\hat{C}_k$ is the identified output matrix, $\delta \boldsymbol{z}_k$ is the perturbation of the identified coordinate system (no physical meaning), and $\delta \hat{\boldsymbol{x}}_k$ is the estimated departure motion in the true coordinate system. First, this model will be directly compared to the true linearized model given by equation (6). This comparison will be done by observing how well both of them are able to replicate the true nonlinear output in the chosen perturbed region. Next, the identified model's ability to preform the station keeping strategy defined in the Problem Statement will be tested.

When it comes to the identified system, after preforming the conversion shown in equation (29), the discrete $A_{k,est}$ at each time step is obtained. By multiplying these together

(as shown in equation (16)), one can obtain the estimated state-transition matrix, Φ_{est}, for the differential corrections algorithm. Note that Φ_{est} is fundamentally different from the previous reference Φ defined in the Problem Statement. The system matrices, $A_{k,est}$, are obtained from linearizing about the nominal orbit instead of the perturbed trajectories found during the iteration process. Interestingly, this means that when using Φ_{est}, the matrix value never changes over the iterations in the differential corrections algorithm for a given time-of-flight. This is not the case for the reference Φ whose value changes after each iteration due to the Jacobian being a function of the state.

Nonetheless, we now have our ground-truth and identified system station-keeping methods defined and can compare their results. Before comparing their results, it is important to note that the differential corrections method is notoriously sensitive to the initial guess for ΔV. An uneducated initial guess can often converge to a state sufficiently far from the desired state on the orbit. For the context of this paper, we wish to observe how well the identified system strategy can station keep compared to the reference. Therefore, how close the final state is to the desired is not of importance. The initial guess for ΔV is taken to be zero for all cases.

Numerical Results

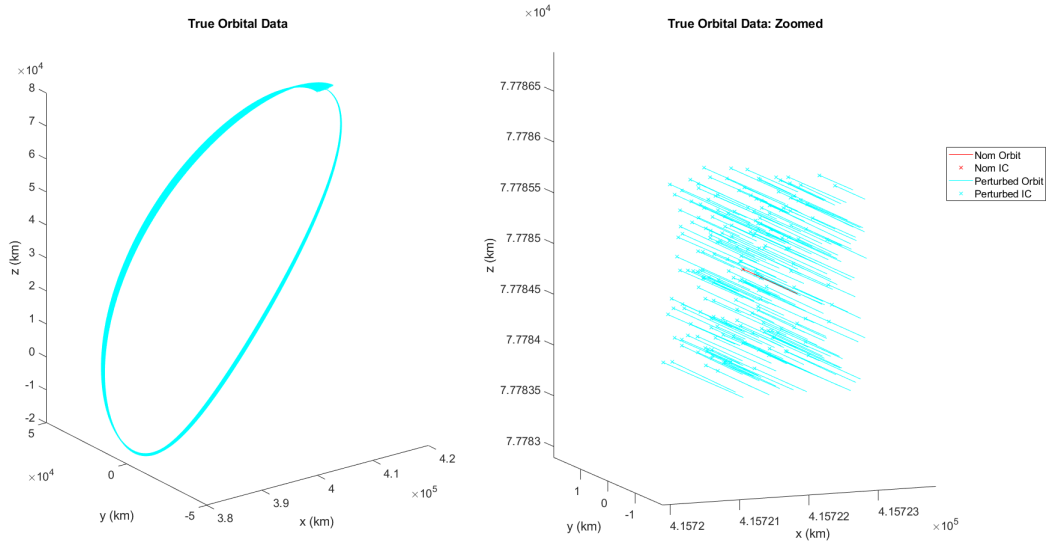

Figure 2: Nominal NRHO and Perturbed Orbits

First, the orbital data was obtained by numerically propagating the CR3BP's dynamics for a set of perturbed initial conditions. This is also often referred to as the "training data". Figure 2 details the orbital data used for the system identification process. The nominal NRHO and its initial condition are shown in red on the right of the figure. The 200 perturbed orbits were obtained by perturbing the nominal initial condition from a uniform distribution with a maximum perturbation magnitude of 1 km and 1 m/s for the initial position and velocity components, respectively. All initial conditions were then propagated

for one nominal time period of 10.25 days. The perturbation of state from the nominal was then utilized in the TVERA/IC process.

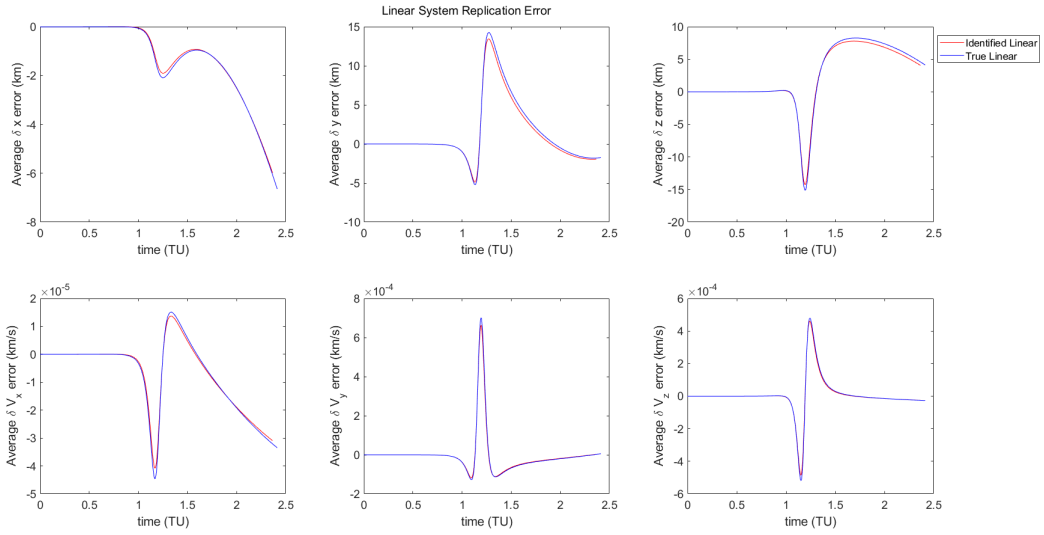

Figure 3: System output replication error

Figure 3 displays how well a time-varying, linear system replicates the nonlinear orbital dynamics. Two linear systems' replication error are shown: the true linearized CR3BP and our identified system from orbital data. The error for each is equal to the corresponding linear system's state propagation minus the nonlinear system's state propagation over one orbital period. One can clearly see that, on average, both system preform approximately the same over time. In general, the dynamics near our nominal NRHO seem to be well approximated by a time-varying, linear system.

The singular value plot shown in Figure 4 has six distinct dominant singular values that correspond to the true six-dimensional system the data was taken from. This meaning our data was sufficiently rich that the overall dynamics are well captured in our identified system. This is further shown in Figure 5 where the coordinate transformation shown in equation (28) was applied. The true A_k and identified $\hat{A}_k$ matrices' eigenvalues are compared over time. Clearly these matrices' eigenvalues do not completely match; however, the identified eigenvalues have a similar structure as the truth. It was not expected for the eigenvalues to match for the identification of a generic nonlinear system, but the similarities bode well for the identified system.

Figure 6 illustrates a differential corrections station-keeping result for a time-of-flight of 6 days. The state starts at the initial condition for a new perturbed orbit found with the same method as the training data for TVERA/IC. The identified system preforms near the same as the ground-truth model. The desired final state was not met completely as mentioned in the problem statement.

In Figure 7, the difference between the final state in the differential corrections algorithm

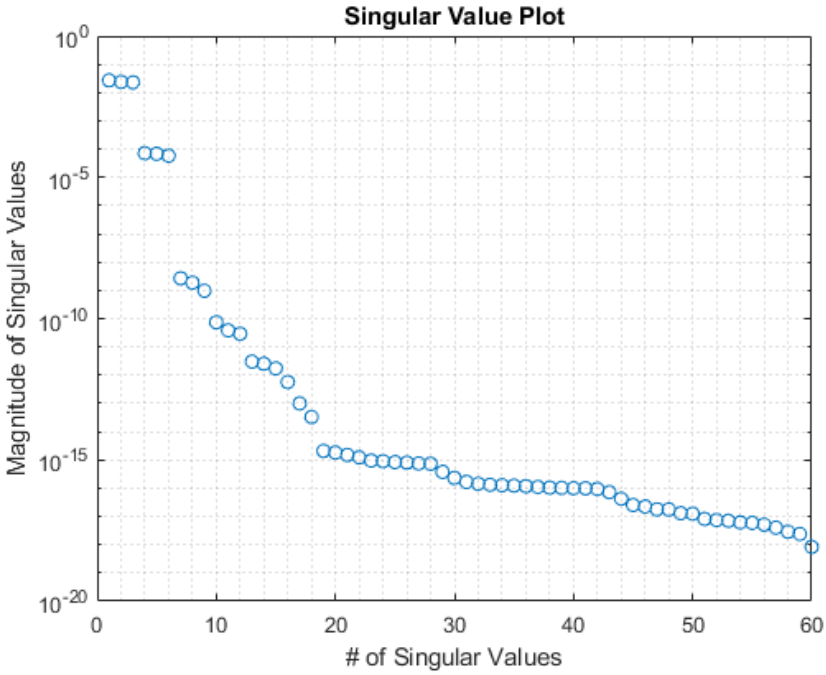

Figure 4: singular value Plot of Hankel matrix

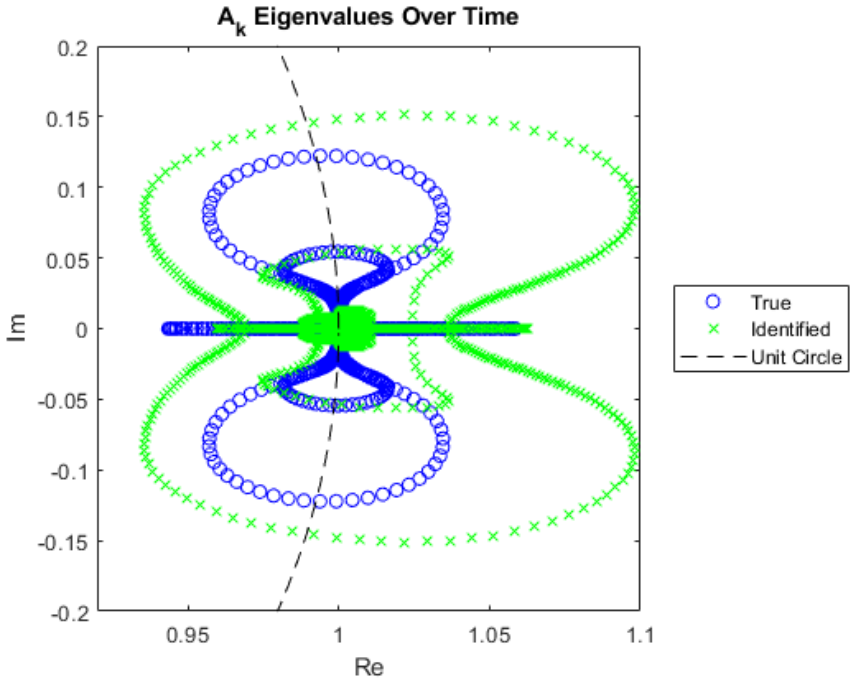

Figure 5: Eigenvalues of A_k over time

for the identified system and ground-truth are plotted as a function of time-of-flight. The time-of-flight varies from 30 minutes to one full orbital period (10.25 days). It is clear that

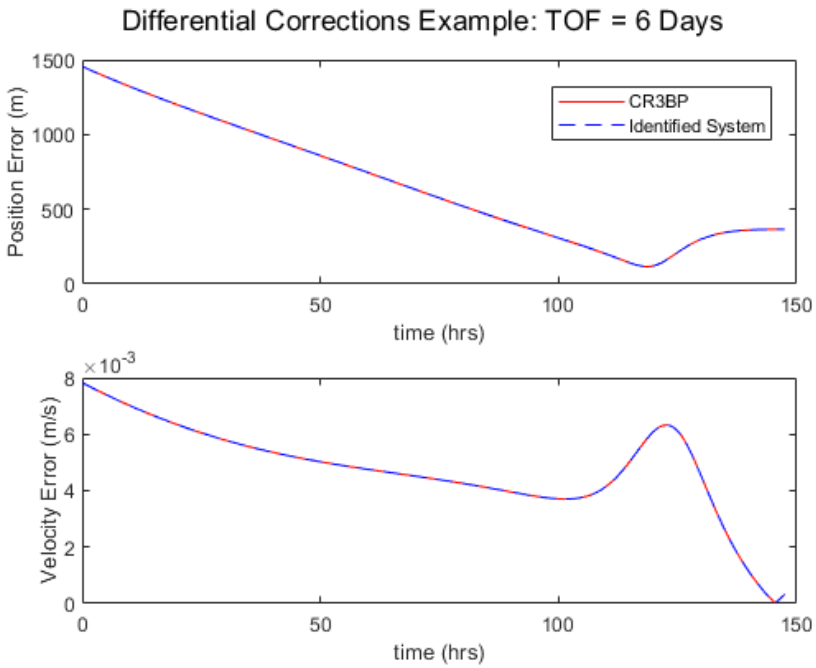

Figure 6: Differential corrections example

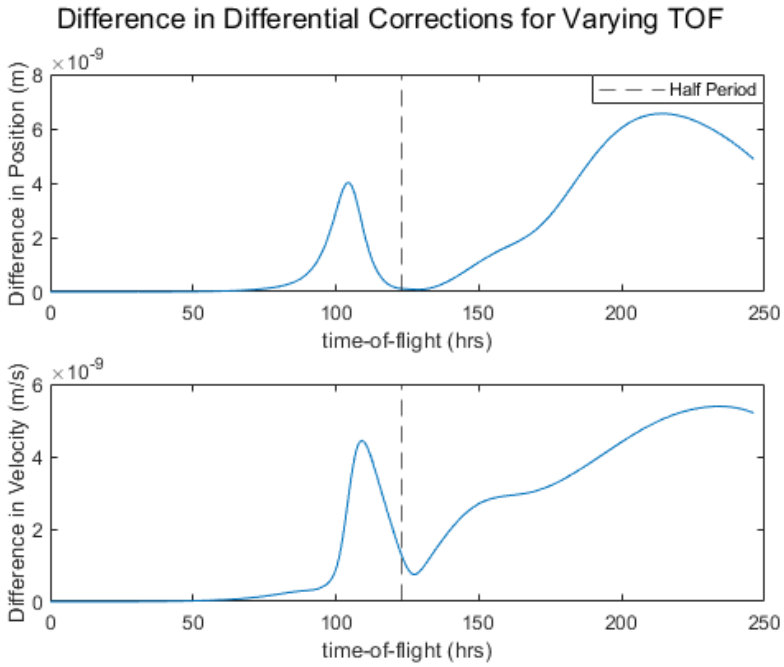

Figure 7: Differential corrections error vs time-of-flight

the identified system preforms just as well as the ground-truth over one revolution. The difference seems to have slight peaks at certain time-of-flights, but further analysis would

be needed for any conclusions on this matter.

Monodromy Matrix Analysis

The Monodromy matrix is used to determine stability of a periodic orbit and is equal to the value of the state-transition matrix after an orbital period. The Monodromy matrix and its eigenvalues were unable to be replicated accurately for cases of high perturbation. Table (1) below shows the estimated Monodromy matrix values as the perturbation magnitudes are decreased to near zero. As the value of the perturbations go to zero, the eigenvalues of the estimated Monodromy matrix converge toward the true values. This convergence is a good sign for the validity of our data-driven modeling.

Table 1: Mondromy matrix eigenvalues as perturbation values are decreased

Reference Eigenvalues	Position Perturbation Velocity Perturbation	1 km 1 m/s	500 m 1 cm/s	50 m 0.1 mm/s	10 m 0.01 mm/s	1 m 0.001 mm/s
-0.6569 + 0.7540i		-7.0867 + 5.7874i	-0.6567 + 0.7541i	-0.6569 + 0.7540i	-0.6568 + 0.7540i	-0.6568 + 0.7540i
-0.6569 - 0.7540i		-7.0867 - 5.7874i	-0.6567 - 0.7541i	-0.6569 - 0.7540i	-0.6568 - 0.7540i	-0.6568 - 0.7540i
0.7707 + 0.6372i		5.6660 + 0.0000i	0.7821 + 0.6188i	0.7707 + 0.6375i	0.7706 + 0.6371i	0.7707 + 0.6370i
0.7707 - 0.6372i		2.1164 + 1.1009i	0.7821 - 0.6188i	0.7707 - 0.6375i	0.7706 - 0.6371i	0.7707 - 0.6370i
1.0000 + 0.0000i		2.1164 - 1.1009i	0.9880 + 0.1662i	1.0209 + 0.0000i	1.0000 + 0.0141i	0.9999 + 0.0183i
1.0000 + 0.0000i		-2.3874 + 0.0000i	0.9880 - 0.1662i	0.9791 + 0.0000i	1.0000 - 0.0141i	0.9999 - 0.0183i

SUMMARY AND FUTURE WORK

In this paper, the efficacy of the initial-condition Eigensystem Realization Algorithm for station keeping purposes was analyzed. A near-rectilinear halo orbit was taken as the nominal, and orbital data was obtained via perturbing the nominal initial condition. From this data, a linear, time-varying model was produced and was determined to be valid in reproducing the nonlinear dynamics over one orbital period. Next, the validity of this identified model was established in the context of impulsive station keeping via the differential corrections method for a fixed-time targeting problem. The identified model performed with the same accuracy as the ground-truth for a variety of time-of-flights over one orbital period. Additionally, the estimated Monodromy eigenvalues were seen to converge to the true values as the perturbations went to near zero.

Future work includes utilizing more realistic orbital data for the modeling, testing different station keeping methods, and analyzing station-keeping around orbits other than near-rectilinear halo orbits. Specifically, station keeping from continuous low-thrust maneuvering is of interest. Other system identification tools must be utilized in this case since there is an input to the system.

ACKNOWLEDGEMENT

This material is based upon work supported jointly by the AFOSR grants FA9550-20-1-0176 and FA9550-22-1-0092.

REFERENCES

[1] Boudad, K., Howell, K., Davis, D.: Near rectilinear halo orbits in cislunar space within the context of the bicircular four-body problem. In: 2nd IAA/AAS SciTech Forum, Moscow, Russia (2019)

[2] Conley, C.: Low energy transit orbits in the restricted three-body problems. SIAM Journal on Applied Mathematics **16**(4), 732–746 (1968)

[3] Gómez, G., Koon, W.S., Lo, M., Marsden, J.E., Masdemont, J., Ross, S.D.: Connecting orbits and invariant manifolds in the spatial restricted three-body problem. Nonlinearity **17**(5), 1571 (2004)

[4] Gómez, G., Mondelo, J.M.: The dynamics around the collinear equilibrium points of the rtbp. Physica D: Nonlinear Phenomena **157**(4), 283–321 (2001)

[5] Guého, D., Singla, P., Huang, D.: Time-varying linear reduced order model for hypersonic aerothermoelastic analysis. In: 2021 AIAA SciTech Forum and Exposition (2021). DOI https://doi.org/10.2514/6.2021-1706

[6] Guého, D., Singla, P., Huang, D.: Application of the time-varying koopman operator for bifurcation analysis in hypersonic aerothermoelasticity. In: 2022 AIAA SciTech Forum and Exposition (2022). DOI https://doi.org/10.2514/6.2022-0655

[7] Guého, D., Singla, P., Majji, M., Juang, J.N.: Advances in system identification: Theory and applications. IEEE Conference on Decision and Control (2021)

[8] Hénon, M.: Numerical exploration of the restricted problem, v. Astronomy and Astrophysics **1**, 223–238 (1969)

[9] HO, B., Kálmán, R.E.: Effective construction of linear state-variable models from input/output functions. at-Automatisierungstechnik **14**(1-12), 545–548 (1966)

[10] Hufenbach, B., Laurini, K., Satoh, N., Lange, C., Martinez, R., Hill, J., Landgraf, M., Bergamasco, A.: International missions to lunar vicinity and surface-near-term mission scenario of the global space exploration roadmap. In: IAF 66th International Astronautical Congress (2015)

[11] Jorba, A., Masdemont, J.: Dynamics in the center manifold of the collinear points of the restricted three body problem. Physica D: Nonlinear Phenomena **132**(1-2), 189–213 (1999)

[12] Juang, J.N.: Applied system identification. Prentice-Hall, Inc. (1994)

[13] Juang, J.N., Pappa, R.S.: An eigensystem realization algorithm for modal parameter identification and model reduction. Journal of guidance, control, and dynamics **8**(5), 620–627 (1985)

[14] Laurini, K.C., Gerstenmaier, W.H.: The global exploration roadmap and its significance for nasa. Space Policy **30**(3), 149–155 (2014)

[15] Majji, M., Juang, J.N., Junkins, J.L.: Time-varying eigensystem realization algorithm. Journal of Guidance, Control, and Dynamics **33**(1), 13–28 (2010). DOI https://doi.org/10.2514/1.45722

[16] Parker, J.S.: Families of low-energy lunar halo transfers. In: AAS/AIAA SpaceFlight Mechanics Conference, AAS06-132, Tampa, Florida, pp. 22–26. Citeseer (2006)

[17] Parker, J.S., Born, G.H.: Direct lunar halo orbit transfers. The Journal of the Astronautical Sciences **56**(4), 441–476 (2008)

[18] Pavlak, T.A.: Trajectory design and orbit maintenance strategies in multi-body dynamical regimes. Ph.D. Dissertation, Purdue University (2013)

[19] Petit, J.M., Hénon, M.: Satellite encounters. Icarus **66**(3), 536–555 (1986)

[20] Rossen, R., Lapidus, L.: Minimum realizations and system modeling. i. fundamental theory and algorithms. AIChE Journal **18**(4), 673–684 (1972)

[21] Rossen, R., Lapidus, L.: Minimum realizations and system modeling: Ii. theoretical and numerical extensions. AIChE Journal **18**(5), 881–892 (1972)

[22] Servadio, S., Arnas, D., Linares, R.: Dynamics near the three-body libration points via koopman operator theory. Journal of Guidance, Control, and Dynamics pp. 1–15 (2022)

[23] Silverman, L.: Realization of linear dynamical systems. IEEE Transactions on Automatic Control **16**(6), 554–567 (1971)

[24] Szebehely, V.: Theory of orbits. yale university (1967)

[25] Tether, A.: Construction of minimal linear state-variable models from finite input-output data. IEEE Transactions on Automatic Control **15**(4), 427–436 (1970)

[26] Villac, B.F., Scheeres, D.J.: Escaping trajectories in the hill three-body problem and applications. Journal of guidance, control, and dynamics **26**(2), 224–232 (2003)

[27] Whitley, R., Landgraf, M., Sato, N., Picard, M., Goodliff, K., Stephenson, K., Narita, S., Gonthier, Y., Cowley, A., Hosseini, S., et al.: Global exploration roadmap derived concept for human exploration of the moon (2017)